Veterinary Microbiology 251 (2020) 108889

Contents lists available at ScienceDirect

Veterinary Microbiology

journal homepage: www.elsevier.com/locate/vetmic

Foot-and-mouth disease virus degrades Rab27a to suppress the exosome-mediated antiviral immune response

Guowei Xu, Shouxing Xu, Xijuan Shi, Chaochao Shen, Dajun Zhang, Ting Zhang, Jing Hou, Keshan Zhang *, Haixue Zheng *, Xiangtao Liu

State Key Laboratory of Veterinary Etiological Biology, National Foot-and-Mouth Disease Reference Laboratory, Lanzhou Veterinary Research Institute, ChineseAcademy of Agriculture Science, Lanzhou, 73004, China

ARTICLE INFO

Keywords:
FMDV
Exosomes
Rab27a
Antiviral immune response
Immune evasion

ABSTRACT

Foot-and-mouth disease (FMD) is a highly contagious infection caused by foot-and-mouth disease virus (FMDV). Exosomes are extracellular vesicles that mediate antiviral immune responses in host cells and could be used by pathogens to evade host cell immune responses. Whether FMDV affects exosome secretion or whether exosomes derived from FMDV-infected cells mediate host cell antiviral immune responses is not yet clarified. In this study, the exosomes were identified and extracted from FMDV-infected PK-15 cells, and it was found that FMDV inhibits exosome secretion. Further investigation revealed that FMDV suppresses exosomes by degrading Rab27a via the autophagy-lysosome pathway. Also, microRNA (miRNA) differential analysis was performed in exosomes, which revealed that miRNA-136 was highly differentially expressed in exosomes and may be the key miRNA that inhibits the proliferation of FMDV. In summary, these results showed that host cells take advantage of exosomes to mediate their antiviral immune response, while FMDV evades exosome-mediated immune responses by degrading the exosome molecular switch, Rab27a.

1. Introduction

Foot-and-mouth disease (FMD) is a harmful contagious disease (Kardjadj, 2017) that causes clinical symptoms, such as blisters and ulcerations in the mouth and hoof. Severe events lead to death of infected animals, such as pigs, cows, or sheep (Grubman and Baxt, 2004). FMD is caused by the foot-and-mouth disease virus (FMDV), which is a single-stranded, positive-strand RNA virus with a genome size of 7.8 kbp that encodes 4 structural proteins P1 (VP1, VP2, VP3, VP4) and 8 non-structural proteins L, P2 (2A, 2B, 2C), and P3 (3A, 3B, 3C, 3D) (Steinberger et al., 2014). Recent studies have recognized exosomes as vital components of viral pathogenesis and immunity. Exosomes are small vesicles with a diameter of 40–150 nm (Jeppesen et al., 2019). The majority of the model cells secrete exosomes that contain multiple bioactive substances, including large amounts of proteins and nucleic acids. The production and secretion of exosomes are regulated by multiple factors. Typically, the production of exosomes involves three endosomal sorting complexes required for transport (ESCRT), lipids, and four-span membrane proteins (Colombo et al., 2014). Additionally, four-span membrane proteins have been shown to belong to a family of proteins that regulate ESCRT-independent endosome sorting. For instance, CD63 protein is highly expressed on the surface of exosomes. Rab protein is a critical molecular switch for intracellular vesicle transport and is involved in the generation, movement, and connection of vesicles with the membrane of the receptor compartment (Wandinger-Ness and Zerial, 2014). Rab11 is the first Rab family protein to be related to exosome secretion (Savina et al., 2002). Advanced studies have proven that Rab27a (Ostrowski et al., 2010) and Rab35 (Hsu et al., 2010) regulate exosome secretion. Some studies have also shown that the downregulation of Rab27a and Rab27b suppress the secretion of exosomes that express CD63, CD81, and MHC class II proteins. Also, the downregulation of Rab27a effectors, Slp4 and Slac2b, inhibit exosome secretion. Pathogenic microorganisms utilize the proteins related to exosome production or secretion to regulate exosome secretion, thereby mediating spontaneous transmission or evading host cell immune responses. For example, murine leukemia virus is a gamma retrovirus that hijacks the host component of the ESCRT for budding (Christina and Reinhild, 2016). Thee exosomes mediate the spread of these biologically active substances between cells (Abdel-Haq, 2019; Anderson et al., 2018; Sun et al., 2018). Also, the exosome components are altered when

* Corresponding authors at: Lanzhou Veterinary Research Institute, Chinese Academy of Agricultural Sciences, No. 1, Xujiaping, Lanzhou 730046, China.
E-mail address: vetzks009@163.com (K. Zhang).

https://doi.org/10.1016/j.vetmic.2020.108889
Received 27 June 2020; Accepted 4 October 2020
Available online 4 November 2020

cells are altered physiologically (Arenaccio et al., 2019; Bai et al., 2019; Cheruiyot et al., 2018).

Reportedly, microRNA (miRNA) in exosomes regulates innate immune responses. The abundance of proteins and nucleic acids contained in the exosomes were significantly changed after infection with a pathogen; also, the amount and type of miRNA were affected (Steinberger et al., 2014). miRNA was first reported in 1993 (Lee et al., 1993) and can be found in most cells. Hitherto, more than 35,000 mature miRNAs have been reported (Liang et al., 2013; Wu et al., 2014). miRNA is a non-coding RNA (ncRNA) gene product involved in the regulation of RNA transcription and translation (Arai et al., 2007) that can bind to miRNA-regulated 3'-untranslated (UTR) to mediate translational regulation (Ling and Calin, 2014). The degree of complementation determines the mechanism by which miRNA regulates mRNA. Gene regulation is the core link that causes changes in biology and phenotype (Lee et al., 2013). Compared to other biologically active substances, miRNA occupies a large proportion of exosomes. Thus, miRNA is considered to be a key component in the biological functions of exosomes (Valadi et al., 2007; Zhang et al., 2016). Previous studies have shown that exosomes mediate the spread of miRNAs (Geis-Asteggiante et al., 2018), facilitating a regulatory role in the biological functions of pathogens and hosts, especially in the host cell immune response.

Exosomes cause the host to produce an effective immune response to a pathogen. Examples of immune responses include the activation of antiviral mechanisms or the transfer of antiviral components (Madison et al., 2015). Depending on the target and the nature of the pathogen, exosomes enhance or limit the viral infections. Many viruses have evolved to escape the host's innate immune response; however, only a few studies have shown the pathogen suppression of the host cell's antiviral immune response by inhibiting exosome secretion. Our previous studies found that exosomes mediate the spread of FMDV (Zhang et al., 2019), but whether FMDV affects the exosome secretion or whether exosomes mediate host cell antiviral immune responses remain unknown.

In this study, we found that FMDV degraded the exosome molecular switch Rab27a protein via the autophagy-lysosome pathway, that miRNA-136 was highly expressed in the exosomes extracted from FMDV-infected cells, with miRNA-136 inhibiting the FMDV proliferation. Interestingly, FMDV did not degrade the Rab27a protein after interfering with miRNA-136 in cells. Herein, we revealed that FMDV suppresses the secretion of exosomes for the first time, which in turn, suppresses the host cell's exosome-mediated antiviral immune response. The current results provided a theoretical basis for the host cell's antiviral immune response and the mechanism by which pathogens avoid immune responses. $TCID_{50}$ and multiplicity of infection (MOI) for FMDV are measured based on the previous studies (Lei et al., 2020; Lowenstein, 2003).

2. Materials and methods

2.1. Cell culture and viruses

In order to obtain the supernatant for exosome extraction, porcine kidney cell line (PK-15) model was used. The cells were cultured in Dulbecco's modified Eagle's medium (Gibco, Waltham, MA, USA) supplemented with 10% fetal bovine serum (FBS), 100 IU/mL penicillin, and 100 mg/mL streptomycin at a temperature of 37 ℃ with 5% CO_2. The FMDV serotype A strain was (A/GDMM/CHA/2013, GenBank number KF450794) was provided by the OIE/national reference laboratory for FMD in China, and the virus strain was isolated from the pig. According to VP1 analysis, it belonged to A/ASIA topotype. PK-15 cells were preserved by the State Key Laboratory of Veterinary Pathogen biology in China. PK-15-CD63-GFP cell line with stable expression of CD63 was constructed by the laboratory. Flag-L, Flag-vp0, Flag-vp1 Flag-vp2, Flag-vp2, Flag-vp3, Flag-2b, Flag-3c, Flag-3d, and empty vector pCAGG were constructed during the experiment, while HA-Rab27a plasmid was constructed by the Laboratory of veterinary Pathogen Biology.

2.2. FMDV infection and cell culture supernatant collection

In order to obtain exosomes secreted by FMDV-infected cells, PK-15 cells were infected with FMDV, and the supernatants were collected at specific time points after infection. Then, PK-15 cells were incubated in a single layer using a 150-mm culture dish (Corning, New York, NY, USA). The culture supernatant was discarded, and the cells were washed with phosphate-buffered saline (PBS) before FBS-free MEM was added. FMDV (A/GDMM/CHA/2013) was injected at the same time as PBS was as a control. After 1 h incubation, the FMDV was discarded and replaced with MEM containing 2% exosome-depleted FBS. Finally, the cell culture supernatant was collected after 24 h.

2.3. Exosome isolation and purification

The collected supernatant was further separated and purified by differential centrifugation 500 $\times g$ for 5 min at 4 ℃ to remove any large fragments and cells, followed by centrifugation again at 2000 $\times g$ for 10 min to further remove the cell debris. Subsequently, the supernatant was collected and spun at 12000 $\times g$ for 45 min to remove cells. Finally, the large vesicles were collected and filtered through a 0.22-μm filter, and the supernatant was collected by ultracentrifugation at 120000 $\times g$ for 2 h (Thermo Scientific Sorvall WX100). The pellet was resuspended in 500 μL PBS. The exosomes were extracted with a CD63 antibody-labeled exosome isolation kit (Miltenyi Biotec, Bergisch Gladbach, Germany).

2.4. Transmission electron microscopy (TEM)

Direct observation based on the morphological characteristics of exosomes is crucial for exosome identification (Shao et al., 2018). Therefore, we used TEM to observe the extracted exosomes (Hitachi H-7000FA, Tokyo, Japan). The exosomes were prepared by incubation with a TEM 200 copper mesh (EMS 80100-Cu US) for 2 min and stained with phosphotungstic acid for 2 min. After drying under an incandescent lamp, the exosomes were viewed with an electron microscope at a voltage of 80 kV.

2.5. Nanoparticle tracking analysis (NTA)

Cells secrete a variety of nanoparticles with varying diameters that can be detected in the supernatant. The size can be used to further identify exosomes. The mean size and size distribution profiles of exosome particles derived from FMDV or mock-infected PK-15 cell culture supernatants after isolation and purification were analyzed as described previously (Fu et al., 2017; Nath Neerukonda et al., 2019). Briefly, exosome samples were diluted before analysis, and the relative concentration was calculated based on the dilution factor. The samples were analyzed using gain adjustments and manual shutter, which resulted in the speeds of 15 or 30 ms, with a shutter speed between 280 and 560. Data were analyzed using NTA 3.2 software (Malvern Panalytical Ltd, Malvern, Worcestershire, UK), and evaluated using a NanoSight NS300 instrument (Malvern Panalytical Ltd). Each sample was analyzed five times, and the average of the counts considered.

2.6. Identification of exosomes by Western blot (WB)

WB was performed using the following protocols. The purified exosomes were lysed using a radio-immunoprecipitation assay buffer (Santa Cruz Biotechnology, Dallas, TX, USA). The clarified lysate was collected by centrifugation, and total protein extract separated on 12% sodium dodecy1 sulfate-polyacrylamide gel electrophoresis (SDS-PAGE). These proteins were transferred to 0.45-μm polyvinylidene difluoride (PVDF) membranes (Millipore, USA) after electrophoresis. Next, the membranes

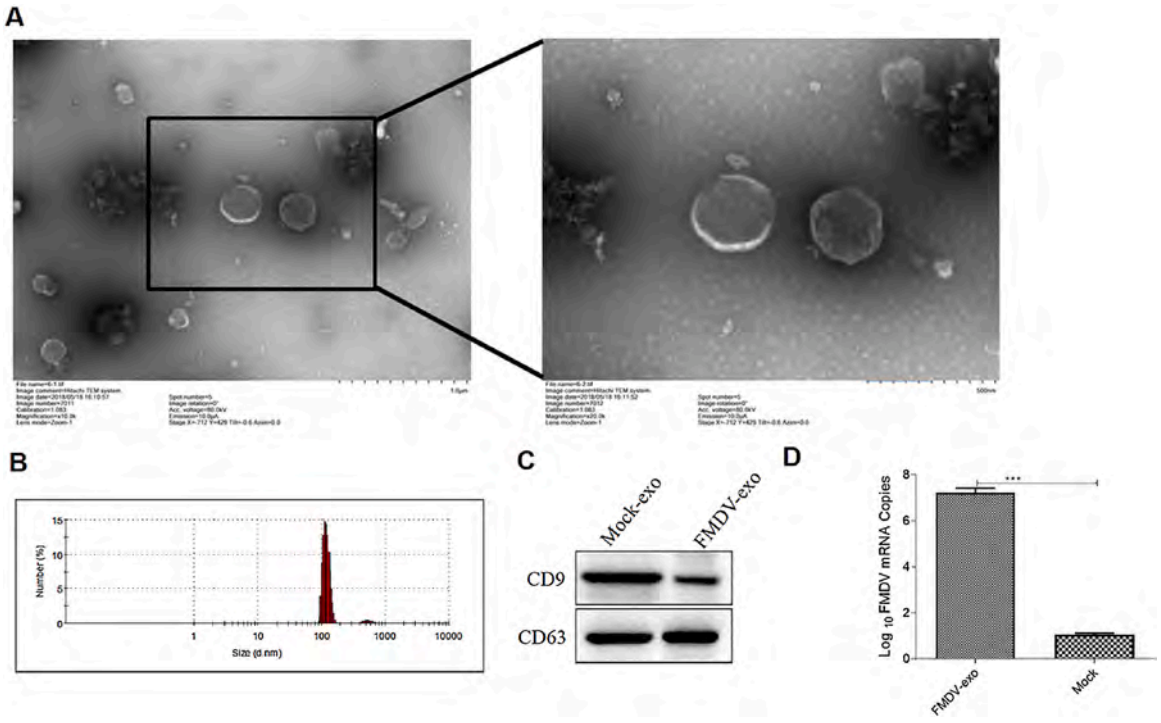

Fig. 1. Isolation and characterization of exosomes extracted from FMDV-infected PK-15 cells. (A) TEM observation of exosome extracted from FMDV-infected PK-15 cells after negative staining. (B) Histogram displaying the mean size and size distribution profile of exosome particles derived from culture supernatants of FMDV-infected PK-15 cells by NTA method. (C) Exosomes were extracted from FMDV-infected PK-15 cells, purified, and identified by WB probe with antibodies directed against Alix and CD63. (D) Detection of *FMDV* mRNA in exosomes by RT-qPCR.

were blocked for 1 h with 10% fat-free milk in Tris-buffered saline containing Tween 20 (TBST). The blots were incubated with primary antibodies, FMDV serotype A, CD63 (Abcam, Cambridge, UK), CD9 (Abcam), Alix (Cell Signaling Technology, Waltham, MA, USA), and Rab27a (Proteintech, Chicago, IL, USA), at 4 ℃ overnight. Subsequently, the membranes were incubated with horseradish peroxidase (HRP)-labeled secondary antibodies for 2 h at room temperature. Finally, the proteins were visualized with enhanced chemiluminescence (ECL) substrate (Bio-Rad Laboratories, Hercules, CA, USA).

2.7. Analysis of miRNA expression profiles

The total RNA or purified sRNA fragments were extracted, and the 3' and 5' linkers were ligated, reverse transcribed into cDNA, and subjected to PCR amplification. Subsequently, the target fragment library was recovered by gelation, and the qualified library was sequenced (Illumina HiSeq^{TM} 2500). The raw data were filtered such that the joints at both ends of the reads were removed. The fragment length with <17 nt and low-quality reads were removed after the initial filtering of the data to obtain high-quality data (clean reads). The ncRNA classification annotations for clean reads judged the expression of the identified miRNA, clustering of miRNA expression, and differential expression between samples miRNA analysis.

2.8. Generation of CD63-GFP stable expression of PK-15 cell lines and FMDV infection

The generation of the stable expression of CD63-GFP in PK-15 cells based on a lentivirus vector was carried out as described previously (Case et al., 1999; Demaison et al., 2002; Natascha et al., 2018). Briefly, the primers of the *CD63* gene (GenBank accession No. XM_005663878.2) were designed and synthesized. The *CD63* gene was cloned onto the multiple cloning site of LvpLVX and termed as Lv-CD63. HEK293T cells (Invitrogen R700-07) were cultured in DMEM containing glucose and glutamine (Gibco), supplemented with 100 μg/mL PenStrep (Gibco) and 10% FBS (Gibco). Plasmids, Lv-pLVX and Lv-CD63, were transfected into HEK293T cells using Lipofectamine2000 in order to package the lentivirus (Thermo Fisher Scientific, Waltham, MA, USA). Subsequently, PK-15 cells infected with packaged lentivirus and stable cell lines (Lv-CD63-PK-15) were selected using limited dilution methods in the presence of 3 μg/mL puromycin . The expression level of the fusion protein CD63 + GFP was examined using RT-qPCR. A microscope was used to observe the green fluorescence signals. Exosome secretion can be enhanced by increasing the CD63 expression (Gauthier et al., 2017; Heikkilä et al., 2016). To evaluate the effect of an FMDV infection on *CD63* gene expression in PK-15 cells, green fluorescence was observed at 24 h after Lv-CD63-PK-15 infection with FMDV.

2.9. Indirect immunofluorescence

The cell density was distributed to 30–60% in a special dish for laser confocal microscopy (the cells were infected with the virus). After washing three times with PBS, the cells were fixed with 4% formaldehyde for 30 min. The cells were permeabilized using 0.2-0.3% Triton X-100 for 10 min, blocked with 5% BSA at room temperature for 1 h, and probed with primary antibody against CD63 overnight at 4 ℃ overnight in the dark. Subsequently, the sections were incubated with GFP fluorescent secondary antibody in 1 × PBST at 37 ℃ for 1 h. Finally, 50–100 μL anti-fluorescence attenuation mounting media was added to the slides (to avoid light), and observed under a laser confocal microscope.

2.10. RNA extraction, reverse transcription, and RT-qPCR

RNase (Sigma) was added to the purified exosomes and incubated at 37 °C for 1 h before RNA extraction. To detect FMDV RNA, total RNA was extracted from exosomes using a total exosome RNA isolation kit (Life Technologies, Carlsbad, CA, USA), according to the manufacturer's instructions. Next, cDNA was synthesized using the respective specific or

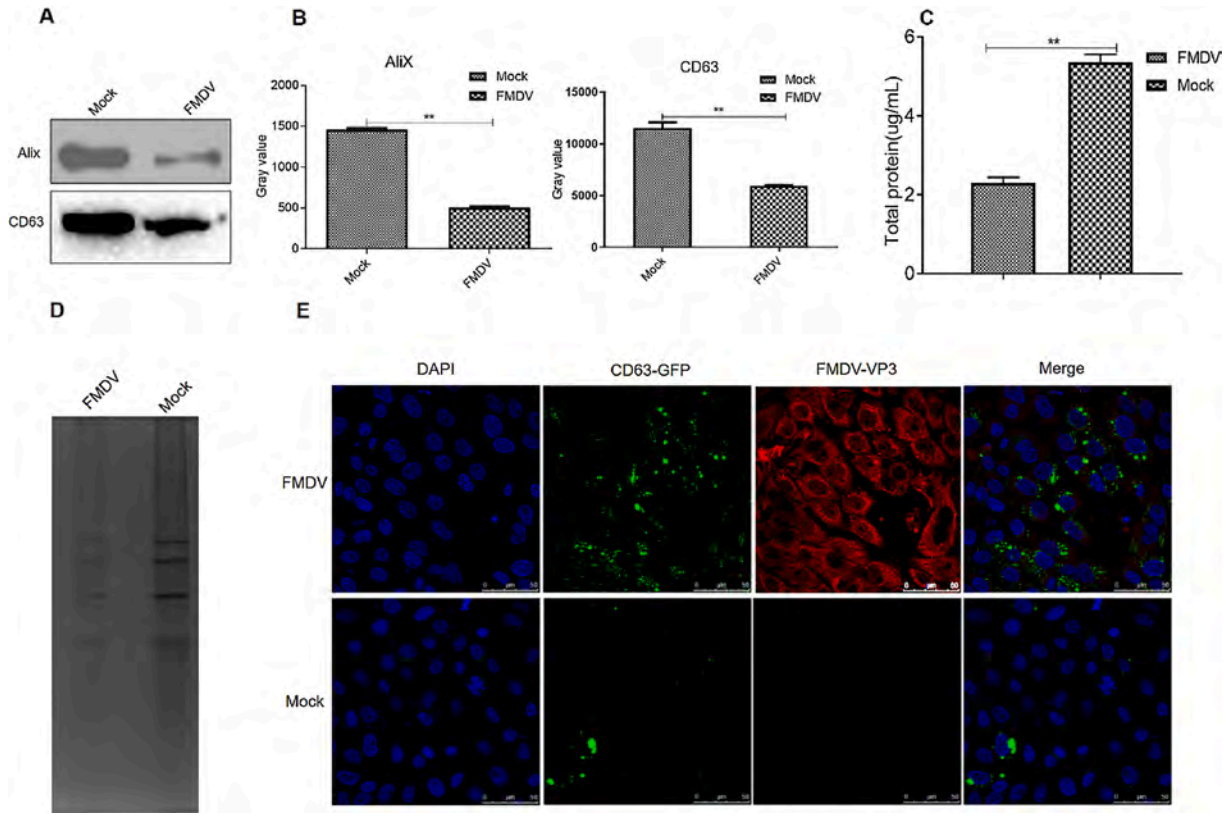

Fig. 2. FMDV infection inhibits the secretion of exosomes. (A) PK-15 cells were infected with FMDV, and an equal volume of PBS was used as the control. The culture supernatant was collected 24 h after FMDV infection, and exosomes were extracted. Finally, the level of exosome marker proteins CD63 and ALIX was detected by WB. (B) The gray-scale scanning analysis of Fig. 2A. (C) PK-15 cells were inoculated with FMDV and an equal volume with controls, and the cell supernatants were collected at 24 h after inoculation. Then ultracentrifugation was performed, and the supernatant purified by CD63 immunomagnetic beads. The total protein concentration was detected by the BCA protein concentration detection method. (D) The extracted exosomes were separated by SDS-PAGE and stained with Coomassie Brilliant Blue. (E) PK-15-CD63-GFP cell line was used to detect whether the exosomes were co-localized with FMDV, and the FMDV-VP3 polyclonal antibody was used for indirect immunofluorescence. The colocalization of FMDV-VP3 (red) and CD63-GFP (green) exosomes was observed under a confocal microscope.

random primers and superscript III reverse transcriptase. The reaction system was prepared using the SYBR® Premix Ex Taq™ (Takara) kit, according to the manufacturer's instructions, and the fluorescence quantitative PCR was conducted according to the Mx3000P operation process. *GAPDH* was used as an internal reference for the relative quantification of the mRNA of different genes. The 20 μL reaction system consisted of 10 μL SYBR Premix Ex Taq II, 0.4 μL upstream primer, 0.4 μL downstream primer, 8.2 μL DEPC water, and 1 μL cDNA and was carried out as follows: predenaturation at 95 ℃ for 3 min and 35 cycles of denaturation at 95 ℃ for 10 s and annealing at 60 ℃ with extension for 34 s.

3. Results

3.1. Extraction and identification of exosomes

The exosomes in the supernatant of PK-15 cells infected with FMDV were enriched by differential centrifugation and ultracentrifugation and purified by CD63 immunomagnetic bead method. In this study, the size of the immunomagnetic beads was about 50 nm. In order to avoid the influence of the magnetic beads, the exosomes were negatively stained with 2% phosphotungstic acid. The cup-shaped lipid bilayer vesicles of the representative exosomes images were observed under transmission electron microscopy (TEM) (Fig. 1A). Then, the exosomes were evaluated using the NTA method, and the particle size was approximately 100 nm, as detected by previous studies (Fig. 1B). Moreover, the exosome maker proteins, Alix and CD63, were detected by WB (Fig. 1C). These results showed that the FMDV-exosomes were successfully isolated and purified from FMDV-infected PK-15 cell culture supernatants. Also, the RT-qPCR test results indicated that FMDV-exo contains FMDV (Fig. 1D).

3.2. FMDV infection inhibits the secretion of exosomes

In order to substantiate the above hypotheses, after inoculating PK-15 cells with FMDV, the cell culture supernatant was collected and exosomes extracted. The levels of exosome marker proteins, CD63 and Alix, were detected and quantitated by WB. These findings suggested that fewer exosomes were isolated from the PK-15 cells with FMDV in comparison to the control group (Fig. 2A and B). To further verify this result, exosomes were extracted from PK-15 cells inoculated with FMDV and purified using CD63 immunomagnetic beads. The protein concentration of the exosomes was measured using the BCA protein concentration detection kit. The total amount of protein was found to be consistent with that of the WB result (Fig. 2C). Coomassie Brilliant Blue staining of the extracted exosomes also implied that the protein content of FMDV-exosomes was lower than that of mock-exosomes (Fig. 2D). In addition, the changes in the number of exosomes were evaluated through laser confocal experiments, and it was observed that the number of CD63-GFP in PK-15 cells was significantly increased after FMDV infection (Fig. 2E), further indicating that FMDV inhibits the secretion of PK-15 cell exosomes and increases the number of intracellular exosomes.

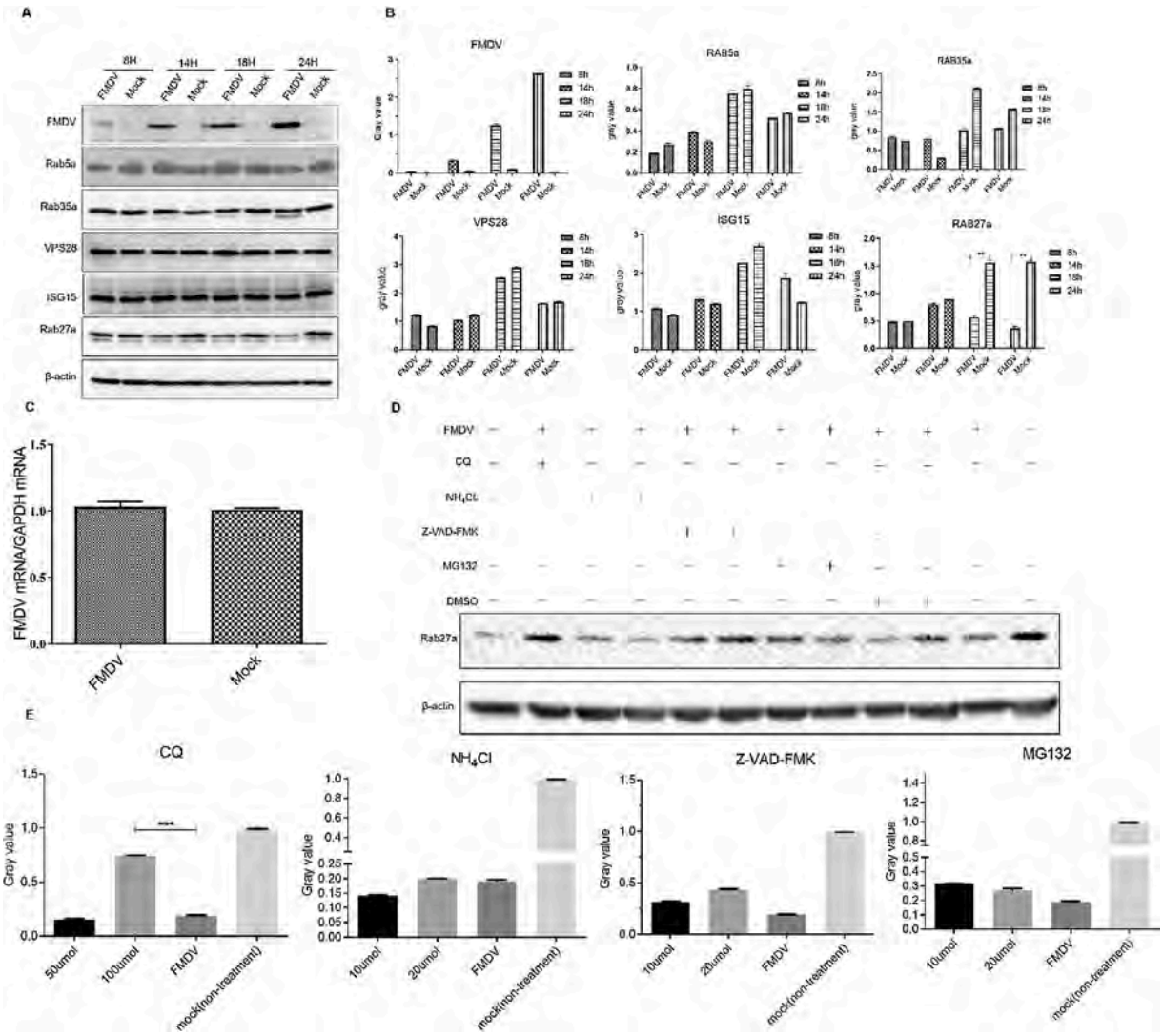

Fig. 3. FMDV degrades Rab27a by autophagy-lysosomal pathway. (A) Effects of FMDV replication on Rab5a, Rab35, VPS28, ISG15, and Rab27a protein levels. The cells were collected at 8, 14, 18, and 24 after FMDV infection of PK-15 cells, and the expression of Rab5a, Rab35, VPS28, ISG15, and Rab27a proteins, related to exosome formation and secretion pathways, was detected by WB; β-actin was used as the internal reference protein. (B) The gray-scale scanning analysis of Fig. 3A. (C) 24 h after FMDV infection of PK-15 cells and PBS (mock) as controls, *FMDV* mRNA was detected. (D) CQ, NH_4Cl, Z-VAD-FMK (caspase-3 inhibitor), and MG132 inhibited autophagy-lysosome, lysosome, caspase, and proteasome pathway of PK-15 cells, respectively, while using an equal volume of DMSO as the control; the cells were then incubated with FMDV. The level of Rab27a was detected, and β-actin was used as an internal reference protein. (E) The gray-scale scanning analysis of Fig. 3D. The data were presented as means ± SD (n = 3 for each group). A significant difference was calculated using two-tailed t-test; $^*P < 0.05$ and $^{**}P < 0.01$.

3.3. *FMDV degrades Rab27a via the autophagy-lysosome pathway*

The data described above proved that FMDV inhibits the secretion of exosomes. In order to elucidate the underlying mechanism, we analyzed the level of exosome-related proteins Rab27a, Rab5a, Rab35, ISG15, and VPS28 in PK-15 cells with FMDV infection by WB. The results showed that FMDV inhibited the expression of Rab27a protein (Fig. 3A) and that the expression of Rab27a was significantly reduced after FMDV infection (Fig. 3B). Previous studies showed that Rab27a plays a critical role in the secretory pathway of exosomes (Wandinger-Ness and Zerial, 2014). Herein, we did not detect any difference in the transcription level of **Rab27a** (Fig. 3C), which led to the speculation that FMDV degrades the Rab27a protein without affecting its transcription level. Next, we used CQ (chloroquine diphosphate salt), NH_4Cl, Z-VAD-FMK (caspase-3 inhibitor), and MG132, which inhibits autophagy-lysosome, lysosome, caspase, and proteasome pathway of PK-15 cells, respectively, while an equal volume of DMSO served as the control. We also incubated FMDV with Rab27a in PK-15 cells and evaluated by WB. The results showed that the level of Rab27a in the CQ group was maximal (Fig. 3D), and that the expression of Rab27a was significantly increased compared with control group according to the gray-scale analysis results (Fig. 3E). The experimental results showed that FMDV degrades the host protein Rab27a via the autophagy-lysosome pathway

3.4. *FMDV-2c degrades Rab27a*

FMDV encodes 4 structural proteins and 8 non-structural proteins. Herein, we aimed to identify the FMDV protein that degrades Rab27a. Hence, the FMDV proteins, L, VP0, VP1, VP2, VP3, 2B, 2C, 3A, 3B, 3C, and 3D were transfected in PK-15 cells, following which, the level of endogenous Rab27a protein was measured by WB. The findings revealed that 2B, 2C, and 3C degrade Rab27a (Fig. 4A), and the expression of 2C was significantly lowest than that of the others. (Fig. 4B). On the other hand, the expression of Rab27a protein decreased with increasing 2C transfected in a dose-dependent manner (Fig. 4C), and the quantitation immunoreactive bands showed that with the increase in the transfection

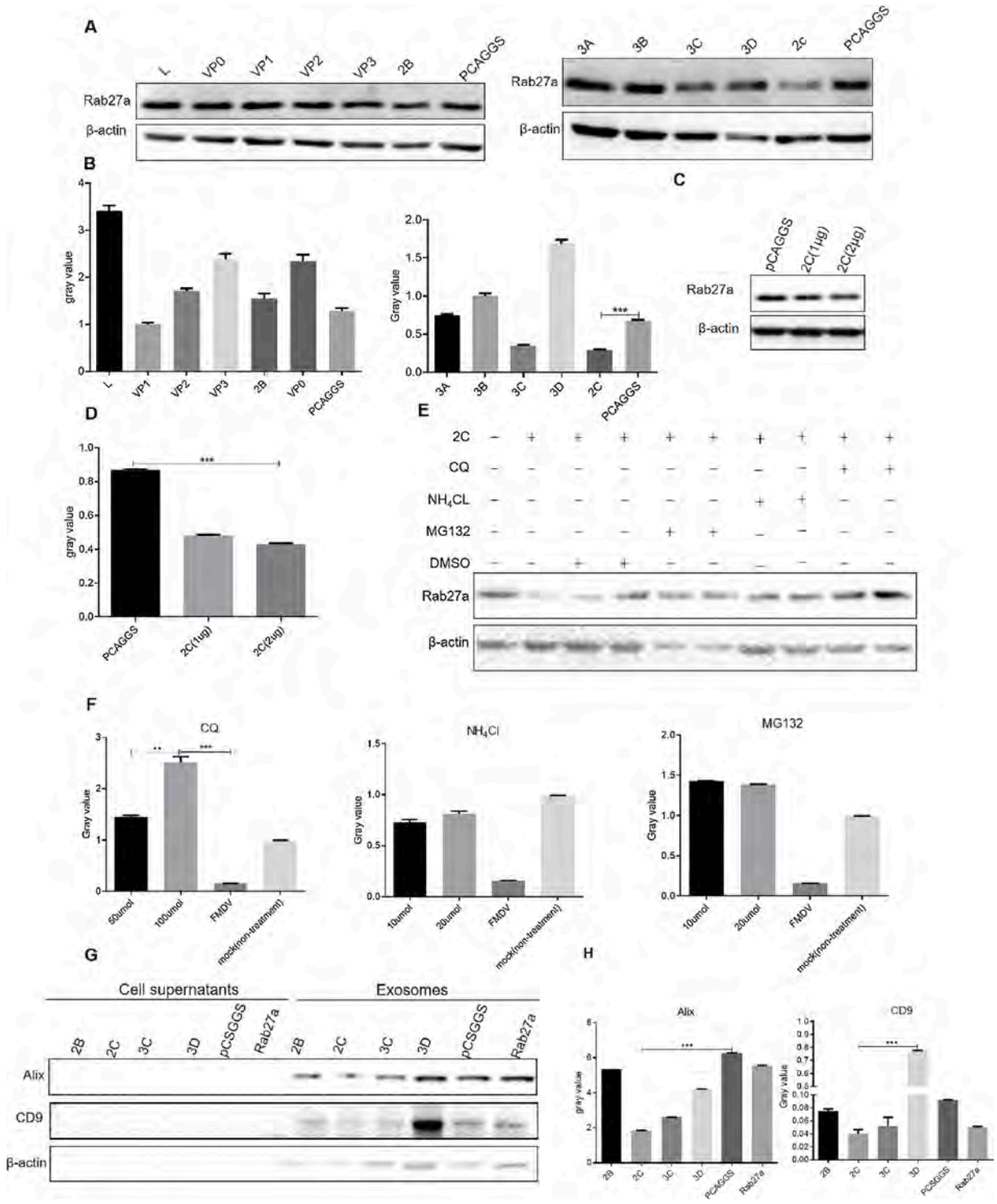

Fig. 4. FMDV-2C degrades Rab27a via the autophagy-lysosome pathway. (A) PK-15 cells were transfected with FMDV protein L, VP0, VP1, VP2, VP3, 2B, 2C, 3A, 3B, 3C, and 3D. After 36 h, the cells were collected to detect the endogenous Rab27a protein by WB. (B) The gray-scale scanning analysis of Fig. 4A. (C) FMDV-2C was transfected with 0, 1, and 2, and the expression of Rab27a protein was detected at 36 h post-transfection. (D) The gray-scale scanning analysis of Fig. 4C. (E) CQ, NH4Cl, Z-VAD-FMK, and MG132 were utilized, and an equal volume of DMSO was used as the control to inhibit autophagy-lysosome pathway, Lysosome, caspase, and proteasome hosts to degrade protein pathways and inoculate FMDV. After collecting the cells, the expression level of Rab27a was detected, and β-actin was used as an internal reference protein. (F) The gray-scale scanning analysis of Fig. 4E. (G) Overexpression of cells was detected in 2B, 2C, 3C, and 3D. After 36 h, the cell supernatant was collected, and exosomes were extracted, and exosome maker proteins Alix and CD9 were detected by WB. (H) The gray-scale scanning analysis of Fig. 4G. All data were represented as means ± SD (n = 3 for each group). A significant difference was calculated using two-tailed t-test; $*P < 0.05$ and $**P < 0.01$.

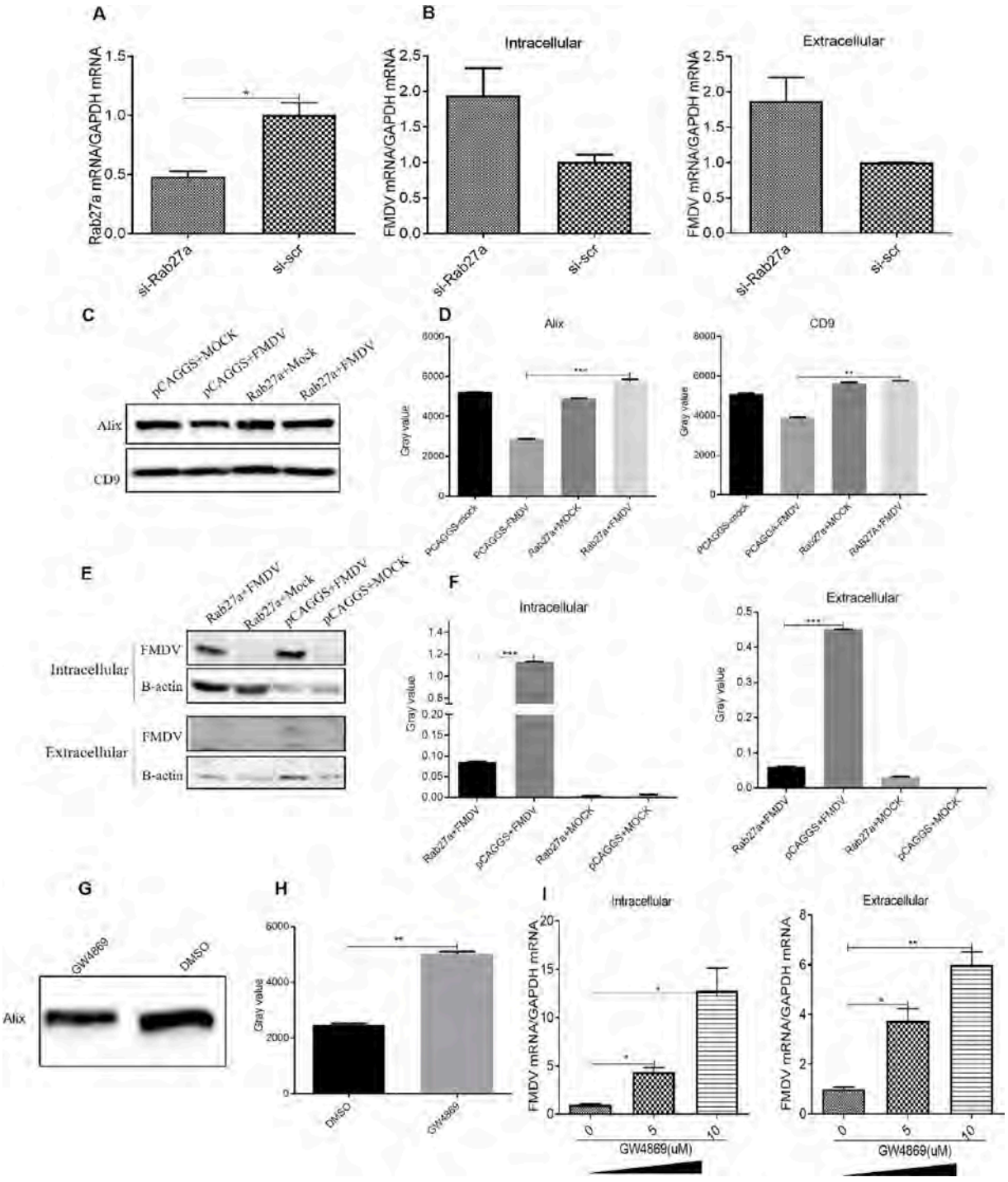

Fig. 5. Interference of Rab27a to promote FMDV replication. (A) FMDV was infected after transfection of si-Rab27a for 36 h in PK-15 cells. After 18 h post-FMDV infection, RT-qPCR was used to detect intracellular *Rab27a* mRNA levels. (B) Intracellular and extracellular *FMDV* mRNA levels were detected. (C) Overexpression of Rab27a inhibits FMDV replication. Rab27a overexpression plasmid and pCAGGS control plasmid were transfected in PK-15 cells, respectively. FMDV and PBS controls were inoculated at 12 h after transfection. Cell supernatants were collected at 24 h after FMDV inoculation, exosomes were extracted, and exosome maker proteins, Alix and CD9 were detected by WB. (D) The gray-scale scanning analysis of Fig. 4C. (E) Overexpression of Rab27a inhibits FMDV replication. Rab27a overexpression plasmid and pCAGGS control plasmid were transfected in PK-15 cells, respectively. FMDV and PBS controls were inoculated at 12 h after transfection. WB was used to detect the expression of intracellular and extracellular FMDV. (F) The gray-scale scanning analysis of Fig. 4E. (G) 24 h after the cells were treated with 10 μmol GW4869, the cell supernatant was collected, and the exosome maker protein Alix was detected by WB. (H) The gray-scale scanning analysis of Fig. 4G. (I) PK-15 cells were treated for 24 h with 0, 5, and 10 μmol GW4869, respectively, with equal volume of DMSO as the control, followed by infection with 1 MOI FMDV. At 18 h after FMDV infection, RT-qPCR was used to detect the *FMDV* mRNA in the intracellular and extracellular regions. All data represent means ± SD (n = 3 for each group). A significant difference was calculated using two-tailed t-test and labeled as $*P < 0.05$ and $**P < 0.01$ in graphs. All data are represented as means±SD (n=3 for each group). A significant difference was calculated using two-tailed t-test and labeled as $*P < 0.05$ and $**P < 0.01$ in graphs.

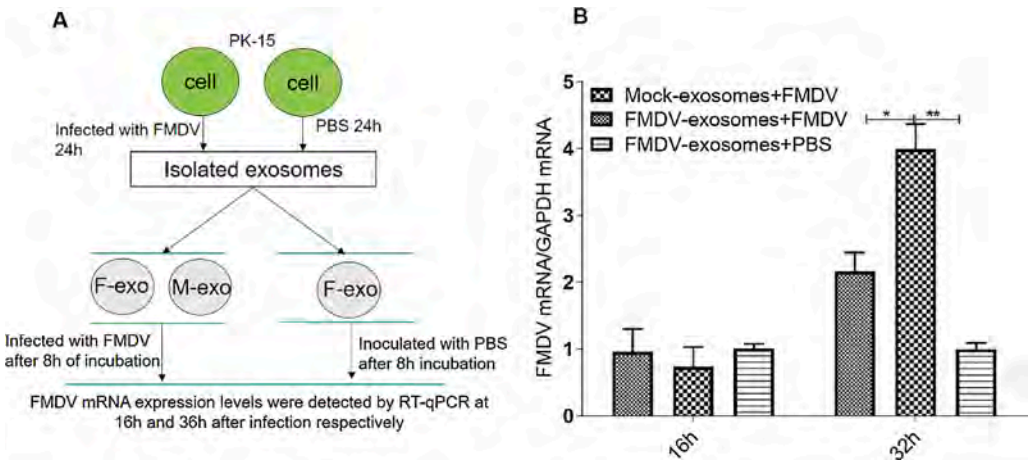

Fig. 6. Exosomes produced by FMDV-infected PK-15 cells inhibit FMDV proliferation. (A) The experimental flowchart of this experiment. As shown in Figure A, FMDV was inoculated in PK-15 cells with the same dose of PBS as the control. The supernatant was collected at 24 h after FMDV inoculation, and exosomes were extracted. Then, the exosomes were incubated with PK-15 cells, and the expression of *FMDV* miRNA in the cells was detected by RT-qPCR after 8 h incubation; cells represent PK-15 cells, F represents FMDV-exo, and M-exo represents Mock-exosomes. (B) PK-15 cells were incubated with exosomes for 8 h and then inoculated with FMDV. Cells were collected at 16 and 32 h after FMDV inoculation, respectively, and *FMDV* RNA copy number was detected. All data are represented as means ± SD (n = 3 for each group). Significant difference was calculated using two-tailed t-test and labeled as $^{*}P < 0.05$ and $^{**}P < 0.01$.

dose of 2C, the expression of Rab27a decreased significantly (Fig. 4D). Subsequently, CQ, NH4Cl, MG132, and an equal volume of DMSO control were used to inhibit the degradation pathway of each protein. It was found that the 2C protein degrades the endogenous Rab27a protein through the autophagy-lysosome pathway, which was similar to that of FMDV (Fig. 4E), and the gray-scale analysis showed an elevated expression of Rab27a in the CQ group (Fig. 4F). After overexpression of 2C, the cell supernatant was collected, and the exosomes were extracted. The exosomes maker proteins, Alix and CD9, were detected by WB, and the cell culture supernatant was used as control after exosome removal. The data revealed that the overexpression of 2C inhibited the secretion of exosomes (Fig. 4G), and the gay-scale analysis also showed that the expression levels of Alix and CD9 were significantly reduced (Fig. 4H). Based on these results, it could be deduced that 2C degrades Rab27a via the autophagy-lysosome pathway.

3.5. Rab27a regulates the proliferation of FMDV

Furthermore, we verified whether interference or overexpression of Rab27a affects the secretion of exosomes (thereby affecting the proliferation of FMDV). Downregulation of Rab27a using RNAi inhibits exosome secretion (Fig. 5A), resulting in a significant increase in the intracellular and extracellular number of FMDV-infected PK-15 cells (Fig. 5B). To further verify the above experimental results, Rab27a was overexpressed in PK-15 cells, and FMDV was inoculated; pCAGGS plasmid and PBS were used in the control group. Then, the exosomes were isolated and the level of Alix and CD9 proteins measured by WB and gray-value. The results showed that the secretion of exosomes was significantly reduced in the pCAGGS + FMDV group as compared to the pCAGGS + MOCK group. Also, no significant difference was detected in the secreted exosomes between the Rab27a + FMDV and Rab27a + MOCK groups (Fig. 5C and D). In addition, WB detected the intracellular and extracellular FMDV expression, and the gray-value of the immunoreactive bands was analyzed, suggesting that the overexpression of Rab27a significantly inhibits FMDV replication (Fig. 5E and F). Furthermore, GW4869 inhibits the formation of exosomes by inhibiting neutral sphingomyelinase 2 (Verderio et al., 2018). After treating PK-15 cells with GW4869, the exosomes were extracted and purified, and the exosome protein Alix detected by WB. The results showed that the number of exosomes was significantly reduced after GW486 treatment as compared to the controls (Fig. 5G and H). Next, PK-15 cells were treated with 0, 5, and 10 μmol GW4869, respectively, with an equivalent volume of DMSO as the control. RT-qPCR revealed that the intracellular and extracellular *FMDV* mRNA was significantly higher than that in the control group (Fig. 5I). The concentration was dose-dependent, indicating that inhibition of the formation of exosomes was beneficial to FMDV replication. Based on these results, we demonstrated that FMDV inhibits the secretion of exosomes.

3.6. FMDV-exosomes inhibit FMDV proliferation

Our previous study showed that exosomes mediate the spread of FMDV (Zhang et al., 2018). To further investigate this phenomenon, exosomes extracted from FMDV-infected PK-15 cells were restored to new PK-15 cells, which were injected with FMDV (Fig. 6A). The results showed that exosomes inhibit the proliferation of FMDV (Fig. 6B), which led us to consider the host perspective, i.e., whether the host cells mediate the antiviral factors through exosomes and inhibit the proliferation of FMDV.

3.7. miRNA-136 in FMDV exosomes inhibit FMDV proliferation

Exosomes contain a large number of miRNAs and play a major role in regulating RAN transcription (Miao, 2017). Herein, we evaluated whether miRNAs are differentially expressed in FMDV-exosomes mediate an antiviral response in host cells. Next, the miRNA expression profiles in exosomes were analyzed. The scatter plot showed that the upregulated miRNA is significantly higher than the downregulated miRNA (Fig. 7A). When the sequence of the common reads among the samples and the specific reads were analyzed, only 15.4% miRNAs were found to be commonly expressed in FMDV-exo and mock-exo (Fig. 7B). The differential expression analysis of miRNAs in exosomes led to a clustered of 59 miRNAs with a differential expression on the heatmap (Fig. 7C). This finding result revealed that FMDV-exosome group clustered differently in the mock-exosomes group. A total of 25 miRNAs showed significant differential expression: 17 upregulated and 8 downregulated (Table 1). The analysis of differentially expressed miRNAs revealed that miRNA-136 is highly expressed in exosomes. Some studies have shown that miRNA-136 is a dual regulator of RIG-I mediated innate immunity, serving as a ligand for RIG-I to enhance innate immunity. This phenomenon suggests that PK-15 cells may enhance their innate antiviral ability by upregulating the expression of

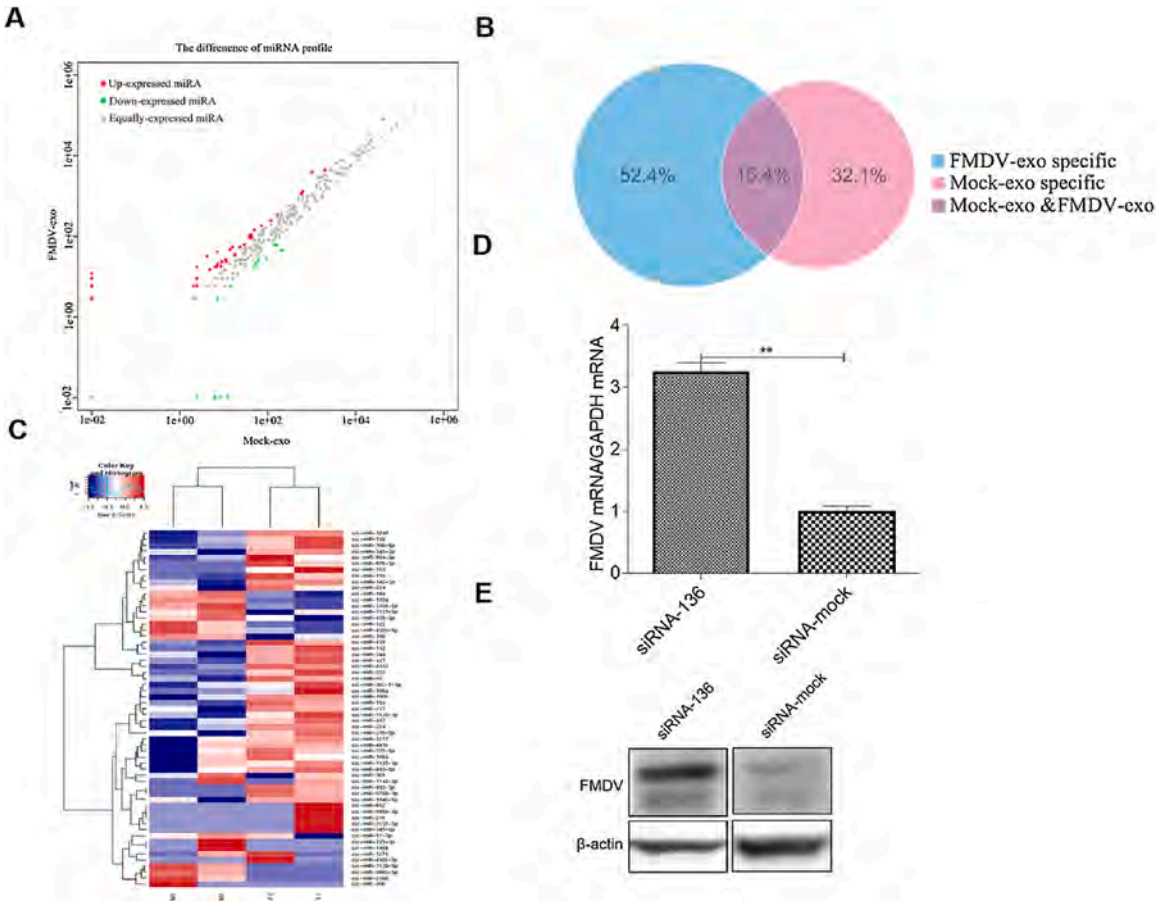

Fig. 7. Complexity of miRNA detected in the FMDV-exosomes and mock-exosomes. (A) Differential expression analysis of miRNA in FMDV-exosome (F1, F2) and mock-exosome (M1, M2) groups, Log2 (fold-change) and scatter plots are used to show the difference in the miRNA expression. Among these, |log2 (fold-change)| and the *P*-value calculated by the edgeR algorithm to determine whether there is a significant difference in the expression of miRNA among the samples. | log2 (fold-change) |≥1 as the threshold, green dots indicate downregulation of miRNA expression, gray dots indicate no change in miRNA expression, and red dots indicate upregulation of miRNA expression. (B) Venn diagram showing the profile of miRNA expressed in FMDV exosomes and mock exosomes. The clean data of different samples and analysis of the reads were compared among the samples and the unique read sequence. (C) Cluster analysis of miRNAs in FMDV-exo and mock-exo heatmap generated by clustering of the 59 most variable miRNAs in FMDV-exosomes and mock-exosomes. Colors represent different normalized sequencing read number as indicated by the color bar (Log2RPM), brick red represents a high expression of miRNA in the sample, and navy blue represents low expression. (D) Relative expression of *FMDV* mRNA in PK-15 cells with transfected siRNA-136, the transfection dose of each miRNA was 200 pmol; the miRNA-mock (irrelevant RNA sequence) group as a control. FMDV with MOI of 1 was inoculated at 36 h after transfection, and *GAPDH* was used as an internal reference gene; the expression levels of miRNA were detected at 12 h after infection with FMDV. (E) At the same time, the protein expression level of Rab27a was detected by WB. All data are represented as means ± SD (n = 3 for each group). A significant difference was calculated using two-tailed t-test and labeled as $^{*}P < 0.05$ and $^{**}P < 0.01$ in the graphs.

miRNA-136. To further prove whether miRNA-136 can affect the proliferation of FMDV, we downregulated the expression of miRNA-136 in PK-15 cells, and examined FMDV at transcription (Fig. 7D) and protein levels (Fig. 7E), respectively. The results showed that interference with miRNA136 promoted the proliferation of FMDV.

4. Discussion

The current results indicated that the anti-FMDV immune response is mediated by exosomes, otherwise, FMDV escapes the immune response by degrading the exosome molecular switch Rab27a protein. Strikingly, exosome-mediated viral transmission is gaining acceptance. For example, some studies have shown that exosomes present in the sera of chronic hepatitis B (CHB) patients contained both HBV nucleic acids and HBV proteins, and transferred HBV to hepatocytes (Yang et al., 2017). Exosomes isolated from PRRSV-infected cells contain viral RNA and proteins (Wang et al., 2018). In the previous studies, we found that exosomes mediate the spread of FMDV (Zhang et al., 2019), while subsequent studies showed that FMDV infected PK-15 cells and inhibited their exosome secretion.

In the process of exosome formation, MVBs sprout inward to form small intraluminal vesicles (ILV) during the transformation of early endosomes to late endosomes, and intraluminal vesicles are released outside the cell as exosomes. Typically, the formation of exosomes involves three pathways: ESCRT, lipids, and four transmembrane proteins (Colombo et al., 2014). Several key proteins, such as Alix, CD63, TSG101, Rab5, Rab11, Rab24, Rab27a, and Rab35, are involved in the production and secretion of exosomes. FMDV inhibits the secretion of exosomes that may be related to the key proteins involved in the formation and secretion of exosomes. FMDV regulates the expression of these proteins through such as to regulate their transcription or degradation. Moreover, this study found that FMDV does not affect the transcription level of exosomal production and secretion-related proteins. However, the expression of the exosomal molecular switch Rab27a protein was significantly reduced compared to control group, indicating that FMDV inhibits the secretion of exosomes by degrading Rab27a. Human parainfluenza virus type 2 (hPIV-2) protein and newly synthesized genomes in the cytoplasm need to be transported to the plasma membrane where budding occurs. hPIV-2 growth is affected by the depletion of Rab27a but not Rab8a or Rab11a (Ohta et al., 2018).

Table 1
Significantly different miRNA data statistics.

MiRNA-ID	up/down	log2(foldchange)	P-value	Significance-Lab
ssc-miR-4332	up	1.9758	1.30E-29	**
ssc-miR-127	up	1.1373	4.80E-10	**
ssc-miR-370	up	1.0332	1.10E-06	**
ssc-miR-95	up	1.0098	1.10E-05	**
ssc-miR-708-5p	up	1.4939	9.70E-04	**
ssc-miR-132	up	1.0684	1.40E-03	**
ssc-miR-451	up	1.0107	1.60E-03	**
ssc-miR-224	up	2.5881	3.20E-03	**
ssc-miR-1249	up	1.432	3.60E-03	**
ssc-miR-34a	up	1.3041	3.70E-03	**
ssc-miR-758	up	1.377	9.50E-03	**
ssc-miR-136	up	1.7948	1.50E-02	*
ssc-miR-497	up	1.773	1.60E-02	*
ssc-miR-145-3p	up	1.1763	2.10E-02	*
ssc-miR-27b-5p	up	2.9793	2.20E-02	*
ssc-miR-664-3p	up	1.2794	2.40E-02	*
ssc-miR-676-3p	up	1.1648	4.00E-02	*
ssc-miR-122	down	−2.2336	2.50E-06	**
ssc-miR-15b	down	−1.3651	7.60E-04	**
ssc-miR-455-3p	down	−1.7938	3.30E-03	**
ssc-miR-450b-5p	down	−1.1568	5.30E-03	**
ssc-miR-18a	down	−1.4293	1.80E-02	*
ssc-miR-130a	down	−1.4563	2.60E-02	*
ssc-miR-1306-5p	down	−1.2353	4.30E-02	*
ssc-miR-7137-5p	down	−1.2292	4.40E-02	*

Note: miRNA-ID represents differentially expressed miRNA; Log2 (Fold Change) represents the logarithmic expression difference multiple with base 2; *P*-value represents the significance level *p*-value; If |log2 Fold Change) |≥1 and *P*-value<0.01, then Significance-Lable is "**"; if |log2(Fold Change)|≥1 and *P*-value<0.05, then Significance-Lable is "**".

The small GTPase Rab27a has been implicated in regulated exosomes, and seems to play a key role in certain membrane trafficking events; for example, herpes simplex virus type 1 (HSV-1) infection of oligodendrocytic cells (Bello-Morales et al., 2012). FMDV may degrade exosomes in many ways, such as autophagy-lysosome, lysosome, caspase, and proteasome, and other host degradation protein pathways. The current study further shows that FMDV is degraded through the autophagy-lysosome pathway, Rab27a.

When exosomes mediate the spread of biological substances between cells, they not only mediate the biologically active substances of pathogenic microorganisms but also contain a variety of biological substances derived from host cells, including substances that regulate host cell immune responses. The studies on dengue virus, human T-cell lymphotropic virus, hepatitis C virus (HCV), and human immunodeficiency virus (HIV) have demonstrated that exosomes isolated from infected cells transmit a variety of regulatory factors (Chahar et al., 2015a). Exosomes released from HCV-infected hepatocytes carry viral RNA and deliver it to plasmacytoid DCs (pDCs) and stimulate TLR7 to produce type I interferon (Dreux et al., 2012). Thus, it is suggested that the suppression of exocrine secretion by FMDV might be related to FMDV-mediated evasion of the immune response of host cells. The biologically active substances contained in exosomes include protein, RNA, miRNA, and other substances. Among them, protein and miRNA account for a large proportion of exosomes, and studies have shown that miRNA regulates the immune response of host cells. miR-423-5p harbored by exosomes could inhibit the replication of the rabies virus (RABV) in MRC-5 cells by blocking the secretion of exosome-promoted RABV infection in MRC-5 cells. This study found that the miRNA expression profiles in FMDV-exo altered significantly and only 15.4% miRNAs were commonly expressed in FMDV-exosomes and mock-exosomes, thereby indicating that FMDV infection reduces the abundance of miRNAs in exosomes secreted by PK-15 cells. The results of this study suggested that these miRNAs with significant changes may be the key factors involved in FMDV-mediated evasion of the host immune response.

Previous studies have shown that miRNA-136 effectively antagonizes the replication of H5N1 influenza A (H5N1 IAV) virus in vitro and that the expression of IL-6 and IFN-β was significantly upregulated after transfecting miRNA-136. Endogenous miRNA acts as the ligand for toll-like receptors and some pattern recognition receptors, with miRNA-136 as an endogenous RIG-I activator (Zhao et al., 2015). This study demonstrated that miRNA-136 is also highly expressed in FMDV-exo and inhibits the proliferation of FMDV. Interfering with the expression of miRNA-136 in PK-15 cells promoted the secretion of exosomes. These findings study suggested that miRNA-136 contained in exosomes is involved in the immune response of host cells.

Due to the limitations of this study, it cannot be explained that FMDV inhibits the secretion of exosomes as the key evidence for FMDV to evade the host immune response. However, for the first time, we demonstrated that FMDV degrades exomolecular switches through the autophagy-lysosome pathway Rab27a, thereby inhibiting exosomal secretion. FMDV infection significantly increases the scale of miRNA-136 that inhibits the proliferation of FMDV in exosomes. Together, the current results indicated that 2C of FMDV degraded Rab27a via the autophagy-lysosome pathway to suppress exosome secretion. Also, FMDV evades exosome-mediated immune responses via host Rab27a, which is a switch for exosome secretion.

Declaration of Competing Interest

The authors declare they have no competing interests.

Acknowledgments

This work was supported by grants from the National Natural Science Foundation of China (31972684). The authors would like to thank the anonymous editors and reviewers for their valuable comments and suggestions that helped improve the quality of this manuscript.

References

Abdel-Haq, H., 2019. Blood exosomes as a tool for monitoring treatment efficacy and progression of neurodegenerative diseases. Neural Regen Res 14, 72–74.
Anderson, M.R., Pleet, M.L., Enose-Akahata, Y., Erickson, J., Monaco, M.C., Akpamagbo, Y., Velluci, A., Tanaka, Y., Azodi, S., Lepene, B., Jones, J., Kashanchi, F., Jacobson, S., 2018. Viral antigens detectable in CSF exosomes from patients with retrovirus associated neurologic disease: functional role of exosomes. Clin Transl Med 7, 24.
Arai, M., Watanabe, A., Kurabayashi, M., 2007. Noncoding RNAs, Emerging Roles in the Regulation of Cardiac Gene Expression. Journal of Cardiac Failure 13, S10.
Arenaccio, C., Chiozzini, C., Ferrantelli, F., Leone, P., Olivetta, E., Federico, M., 2019. Exosomes in Therapy: Engineering, Pharmacokinetics and Future Applications. Curr Drug Targets 20, 87–95.
Bai, X., Guo, Y., Shi, Y., Lin, J., Tarique, I., Wang, X., Vistro, W.A., Huang, Y., Chen, H., Haseeb, A., Yang, P., Chen, Q., 2019. In vivo multivesicular bodies and their exosomes in the absorptive cells of the zebrafish (Danio Rerio) gut. Fish Shellfish Immunol 88, 578–586.
Case, S.S., Price, M.A., Jordan, C.T., Yu, X.J., Wang, L., Bauer, G., Haas, D.L., Xu, D., Stripecke, R., Naldini, L., Kohn, D.B., Crooks, G.M., 1999. Stable transduction of quiescent CD34(+)CD38(-) human hematopoietic cells by HIV-1-based lentiviral vectors. In Proc Natl Acad Sci U S A 2988–2993.
Chahar, H.S., Bao, X., Casola, A., 2015a. Exosomes and Their Role in the Life Cycle and Pathogenesis of RNA Viruses.
Cheruiyot, C., Pataki, Z., Ramratnam, B., Li, M., 2018. Proteomic Analysis of Exosomes and Its Application in HIV-1 Infection. Proteomics Clin Appl 12, e1700142.
Christina, B., Reinhild, P., 2016. ESCRT Requirements for Murine Leukemia Virus Release. Viruses 103-.
Colombo, M., Raposo, G., Thery, C., 2014. Biogenesis, secretion, and intercellular interactions of exosomes and other extracellular vesicles. Annu Rev Cell Dev Biol 30, 255–289.
Demaison, C., Parsley, K., Brouns, G., Scherr, M., Battmer, K., Kinnon, C., Grez, M., Thrasher, A.J., 2002. High-level transduction and gene expression in hematopoietic repopulating cells using a human imunodeficiency virus type 1-based lentiviral vector containing an internal spleen focus forming virus promoter. Human Gene Therapy 13, 803–813.
Dreux, M., Garaigorta, U., Boyd, B., Decembre, E., Chung, J., Whitten-Bauer, C., Wieland, S., Chisari, F.V., 2012. Short-range exosomal transfer of viral RNA from infected cells to plasmacytoid dendritic cells triggers innate immunity. Cell host & microbe 12, 558–570.

Fu, Y., Zhang, L., Zhang, F., Tang, T., Zhou, Q., Feng, C., Jin, Y., Wu, Z., 2017. Exosome-mediated miR-146a transfer suppresses type I interferon response and facilitates EV71 infection. PLoS Pathog 13, e1006611.
Gauthier, S.A., Pérez-González, R., Sharma, A., Huang, F.K., Alldred, M.J., Pawlik, M., Kaur, G., Ginsberg, S.D., Neubert, T.A., Levy, E., 2017. Enhanced exosome secretion in Down syndrome brain - a protective mechanism to alleviate neuronal endosomal abnormalities. Acta Neuropathologica Communications 65.
Geis-Asteggiante, L., Belew, A.T., Clements, V.K., Edwards, N.J., Ostrand-Rosenberg, S., El-Sayed, N.M., Fenselau, C., 2018. Differential Content of Proteins, mRNAs, and miRNAs Suggests that MDSC and Their Exosomes May Mediate Distinct Immune Suppressive Functions. J Proteome Res 17, 486–498.
Grubman, M.J., Baxt, B., 2004. Foot-and-mouth disease. Clin Microbiol Rev 17, 465–493.
Heikkilä, O., Ryödi, E., Hukkanen, V., 2016. γ134.5 neurovirulence gene of herpes simplex virus type 1 modifies the exosome secretion profile in epithelial cells. J Virol 10981.
Hsu, Chieh, Morohashi, Yuichi, Yoshimura, Shin-ichiro, Manrique-Hoyos, Natalia, Jung, SangYong, Lauterbach, Marcel A., 2010. Regulation of exosome secretion by Rab35 and its GTPase-activating proteins TBC1D10A-C. The Journal of cell biology.
Jeppesen, D.K., Fenix, A.M., Franklin, J.L., Higginbotham, J.N., Zhang, Q., Zimmerman, L.J., Liebler, D.C., Ping, J., Liu, Q., Evans, R., Fissell, W.H., Patton, J.G., Rome, L.H., Burnette, D.T., Coffey, R.J., 2019. Reassessment of Exosome Composition. Cell 177 (428-445), e418.
Kardjadj, M., 2017. Foot-and-mouth disease (FMD) in the Maghreb and its threat to southern European countries. Tropical Animal Health & Production 49, 1–3.
Lee, K.H., Kim, S.H., Lee, H.R., Kim, W., Kim, D.Y., Shin, J.C., Yoo, S.H., Kim, K.T., 2013. MicroRNA-185 oscillation controls circadian amplitude of mouse Cryptochrome 1 via translational regulation. Mol Biol Cell 24, 2248–2255.
Lee, R.C., Feinbaum, R.L., Ambros, V., 1993. The C. elegans heterochronic gene lin-4 encodes small RNAs with antisense complementarity to lin-14. Cell 75, 843–854.
Lei, C., Yang, J., Hu, J., Sun, X., 2020. On the Calculation of TCID50 for Quantitation of Virus Infectivity. Virol Sin.
Liang, P., Feng, B., Zhou, X.G., Gao, X.W., 2013. Identification and Developmental Profiling of microRNAs in Diamondback Moth, Plutellaxylostella (L.). Plos One 8.
Ling, H., Calin, G.A., 2014. Chapter 25 - The Role of MicroRNAs and Ultraconserved Non-Coding RNAs in Cancer. In: Dellaire, G., Berman, J.N., Arceci, R.J. (Eds.), Cancer Genomics. Academic Press, Boston, pp. 435–447.
Lowenstein, P.R., 2003. Virology and immunology of gene therapy, or virology and immunology of high MOI infection with defective viruses. Gene Ther 10, 933–934.
Madison, M.N., Jones, P.H., Okeoma, C.M., 2015. Exosomes in human semen restrict HIV-1 transmission by vaginal cells and block intravaginal replication of LP-BM5 murine AIDS virus complex. Virology 482, 189–201.
Miao, X.Y., 2017. Recent advances in understanding the role of miRNAs in exosomes and their therapeutic potential. Journal of Integrative Agriculture 16, 753–761.
Natascha, Gödecke, Hansjörg, Hauser, Dagmar, Wirth, 2018. Stable Expression by Lentiviral Transduction of Cells. Methods in molecular biology.
Nath Neerukonda, S., Egan, N.A., Patria, J., Assakhi, I., Tavlarides-Hontz, P., Modla, S., Munoz, E.R., Hudson, M.B., Parcells, M.S., 2019. Comparison of exosomes purified via ultracentrifugation (UC) and Total Exosome Isolation (TEI) reagent from the serum of Marek's disease virus (MDV)-vaccinated and tumor-bearing chickens. J Virol Methods 263, 1–9.
Ohta, K., Matsumoto, Y., Nishio, M., 2018. Rab27a facilitates human parainfluenza virus type 2 growth by promoting cell surface transport of envelope proteins. Med Microbiol Immunol.
Ostrowski, M., Carmo, N.B., Krumeich, S., Fanget, I., Raposo, G., Savina, A., Moita, C.F., Schauer, K., Hume, A.N., Freitas, R.P., Goud, B., Benaroch, P., Hacohen, N., Fukuda, M., Desnos, C., Seabra, M.C., Darchen, F., Amigorena, S., Moita, L.F., Thery, C., 2010. Rab27a and Rab27b control different steps of the exosome secretion pathway. Nature cell biology 12 (19-30), 11–13.
Savina, A., Vidal, M., Colombo, M.I., 2002. The exosome pathway in K562 cells is regulated by Rab11. Journal of Cell Science 115, 2505–2515.
Steinberger, J., Grishkovskaya, I., Cencic, R., Juliano, L., Juliano, M.A., Skern, T., 2014. Foot-and-mouth disease virus leader proteinase: structural insights into the mechanism of intermolecular cleavage. Virology 468-470, 397–408.
Sun, Z., Yang, S., Zhou, Q., Wang, G., Song, J., Li, Z., Zhang, Z., Xu, J., Xia, K., Chang, Y., Liu, J., Yuan, W., 2018. Emerging role of exosome-derived long non-coding RNAs in tumor microenvironment. Mol Cancer 17, 82.
Valadi, H., Ekstrom, K., Bossios, A., Sjostrand, M., Lee, J.J., Lotvall, J.O., 2007. Exosome-mediated transfer of mRNAs and microRNAs is a novel mechanism of genetic exchange between cells. Nature cell biology 9, 654–U672.
Verderio, C., Gabrielli, M., Giussani, P., 2018. Role of sphingolipids in the biogenesis and biological activity of extracellular vesicles. Journal of lipid research.
Wandinger-Ness, A., Zerial, M., 2014. Rab proteins and the compartmentalization of the endosomal system. Cold Spring Harb Perspect Biol 6, a022616.
Wang, T., Fang, L., Zhao, F., Wang, D., Xiao, S., 2018. Exosomes Mediate Intercellular Transmission of Porcine Reproductive and Respiratory Syndrome Virus. J Virol 92.
Wu, J., Zhu, H., Song, W., Li, M., Liu, C., Li, N., Tang, F., Mu, H., Liao, M., Li, X., Guan, W., Li, X., Hua, J., 2014. Identification of conservative microRNAs in Saanen dairy goat testis through deep sequencing. Reprod Domest Anim 49, 32–40.
Yang, Y., Han, Q., Hou, Z., Zhang, C., Tian, Z., Zhang, J., 2017. Exosomes mediate hepatitis B virus (HBV) transmission and NK-cell dysfunction. Cellular & molecular immunology 14, 465–475.
Zhang, D., Lee, H., Zhu, Z., Minhas, J.K., Jin, Y., 2016. Enrichment of selective miRNAs in exosomes and delivery of exosomal miRNAs in vitro and in vivo. Am J Physiol Lung Cell Mol Physiol 312 ajplung.00423.02016.
Zhang, K., Lu, B., Liu, H., Zhao, J., Zheng, H., Liu, X., 2018. Adverse Effects of Inactivated Foot-and-Mouth Disease Vaccine—Possible Causes Analysis and Countermeasures. World Journal of Vaccines 08, 81–88.
Zhang, K., Xu, S., Shi, X., Xu, G., Shen, C., Liu, X., Zheng, H., 2019. Exosomes-mediated transmission of foot-and-mouth disease virus in vivo and in vitro. Vet Microbiol 233, 164–173.
Zhao, L., Zhu, J., Zhou, H., Zhao, Z., Zou, Z., Liu, X., Lin, X., Zhang, X., Deng, X., Wang, R., 2015. Identification of cellular microRNA-136 as a dual regulator of RIG-I-mediated innate immunity that antagonizes H5N1 IAV replication in A549 cells. Sci Rep-Uk 5, 14991.